Current Opinion in Colloid & Interface Science 26 (2016) 28–40

Contents lists available at ScienceDirect

Current Opinion in Colloid & Interface Science

journal homepage: www.elsevier.com/locate/cocis

Single polymer dynamics of topologically complex DNA

Danielle J. Mai [a], Charles M. Schroeder [a,b,*]

[a] Department of Chemical and Biomolecular Engineering, University of Illinois at Urbana-Champaign, Roger Adams Laboratory, 600 South Mathews Avenue, Urbana, IL, 61801, United States
[b] Center for Biophysics and Quantitative Biology, University of Illinois at Urbana-Champaign, Roger Adams Laboratory, 600 South Mathews Avenue, Urbana, IL 61801, United States

ARTICLE INFO

Article history:
Received 22 April 2016
Received in revised form 24 August 2016
Accepted 29 August 2016
Available online 11 September 2016

Keywords:
Polymer
DNA
Architecture
Topology
Rings
Knots
Branched polymers
Single molecule

ABSTRACT

Single molecule studies allow for the direct observation of polymer dynamics in dilute and concentrated solutions, thereby revealing polymer chain conformations and molecular sub-populations that may be obscured in ensemble-level measurements. Over the past two decades, researchers have used DNA as a model system to study polymer dynamics at the molecular level. The vast majority of studies have focused on linear DNA molecules; however, researchers have recently begun to study polymers with complex topologies and architectures at the single molecule level. Here, we explore recent work in single polymer dynamics focused on topologically complex DNA, including knots, ring polymers, and branched polymers. Experimental, computational, and theoretical advances have enabled in-depth studies of topologically complex DNA, with recent efforts focused on complex molecular conformations, intermolecular interactions, and topology-dependent dynamics. In this article, we highlight recent work aimed at understanding the interplay between molecular-scale behavior and the emergent properties of polymeric materials.

1. Introduction

Topological constraints in polymeric materials have long been considered as fascinating and challenging problems in polymer physics [1–3]. In mathematics, topology refers to the preservation of spatial properties upon continuous deformation such as stretching or bending. In some cases, shape and conformation are independent of topology, and topological constraints arise from the uncrossability of physically connected elements, such as entangled polymer chains [1]. In the field of polymer science, topology adopts a broad definition, generally referring to intramolecular shape (e.g. branched or circular polymers) and/or intermolecular interactions (e.g. entangled polymers), both of which are impacted by polymer sequence, molecular weight, architecture, and chain connectivity [4]. These microstructural and physical features provide non-chemical handles that can be leveraged to drive structure–property relationships in polymeric materials. For example, polymers with brush-like topologies have recently been used to prepare soft, solvent-free networks [5•]. Here, tuning the polymer branch length and density resulted in single-component materials with superior elasticity and extensibility compared to designer hydrogels for biological applications.

Molecular-scale connectivity is known to play a key role in determining the relationship between molecular topology and the emergent physical properties of polymeric materials. Rheological studies of branched polymers with architectural dispersity have revealed the sensitivity of viscoelastic response to topological impurities in entangled polymers [6•]. Similarly, conflicting reports of ring polymer melt viscoelasticity have been attributed to trace linear impurities [7]. Topological defects in networks, such as dangling ends or loops, directly impact the mechanical properties of gels, in some cases preventing gel formation altogether [8]. Despite numerous advances in chemical synthesis, a grand challenge remains in achieving large-scale, precise control over complex polymer sequences and architectures [9•].

In nature, these challenges are overcome by dynamic regulation of microscopic topological events in biological macromolecules with remarkably high frequency and precision. Biopolymers such as deoxyribonucleic acid (DNA) undergo knotting and unknotting events, circularization and supercoiling, or the formation of branched junctions for replication [10]. These topological transitions are aided by the double stranded and double-helical nature of DNA strands, which imparts an intrinsic twist (or combination of twist and writhe) along DNA backbones. In living systems, DNA topology is regulated by a class of enzymes called topoisomerases, which are known to generate transient breakages along DNA strands to alter topology while preserving sequence [11]. Single molecule techniques have enabled insightful biophysical studies of DNA topology, uncovering the structural dynamics of individual Holliday junctions [12] and mechanisms for supercoiling [13]. Nevertheless, the dynamics of polymers with complex topologies has not yet been fully characterized using single polymer techniques, and this nascent area of research is a particularly exciting new direction in the field.

In this review, we highlight the use of DNA to study the impact of topology on single polymer dynamics. This review covers recent experimental, computational, and theoretical advances in knotted, circular,

* Corresponding author.
E-mail address: cms@illinois.edu (C.M. Schroeder).

http://dx.doi.org/10.1016/j.cocis.2016.08.003
1359-0294/

and branched polymers. DNA serves as a powerful system for single polymer dynamics, in particular due to an established understanding of the physical properties and preparation methods, including facile fluorescent labeling, compatibility with aqueous buffers, and templated synthesis of monodisperse polymers. For single molecule studies of linear DNA dynamics, we refer readers to recent reviews on DNA in hydrodynamic flows [14], electrophoresis [15], and confinement [16]. In this article, we focus on the physics of polymer chain topology, namely its influence on single polymer dynamics at equilibrium and under non-equilibrium flows.

2. DNA knots

Knots are central to the theory of mathematical topology [17], and naturally occurring knots have been discovered in various macromolecules and biopolymers [18]. Knots can also be generated by chemical and physical means, wherein the latter has been studied in the context of knots in single polymers. Rigorous definitions of knots exist only for closed structures, but knotting is observed on both open chains and closed loops in single DNA molecules. Knots may be classified in several ways, most commonly using the Alexander–Briggs notation [17]. Here, a knot is first designated by the number of self-crossings, followed by an arbitrary index to distinguish topologically different knots with the same number of crossings. A single loop with no knots (the "unknot") is designated 0_1, and the simplest non-trivial knot (trefoil) is labeled 3_1. Knot complexity and topological uniqueness increase with the crossing number, such that five crossings give rise to two unique knots (5_1 and 5_2), six crossings to three unique knots (6_1, 6_2, 6_3), seven crossings to seven knots, and so on.

Further classifications for knots include torus, twist, and chiral or achiral knots. Torus knots encompass the family of knots with notation $(2n + 1)_1$; these knots can be represented as closed curves on the surface of a torus. Twist knots are an example of supercoiling and are formed by twisting and folding a loop repeatedly before closing its ends. Finally, chirality describes whether a knot is equivalent to its mirror image.

Although natural occurrences of numerous knot topologies have been detected and classified since the late 1970s [18], the first demonstration of actively tying a molecular knot was not reported until 1999 [19]. The ability to simultaneously generate and visualize knots using optical tweezers enabled a seminal paper quantifying the behavior of knots in fluorescently labeled DNA molecules [20•]. In this paper, Quake and coworkers observed a strong influence of topology on the size and mobility of single knots in DNA (Fig. 1a–d). Perhaps not surprisingly, knots with increasingly complex topologies diffused more slowly along DNA. Calculations of drag coefficients for single knots correlated with predictions for ideal, tight knots, thereby demonstrating the validity of DNA as a robust polymeric system for studying knotting phenomena.

These findings further sparked broad interest in the physics of knotted polymer molecules, which encompasses a wide design space, from equilibrium properties to topology-dependent behavior to

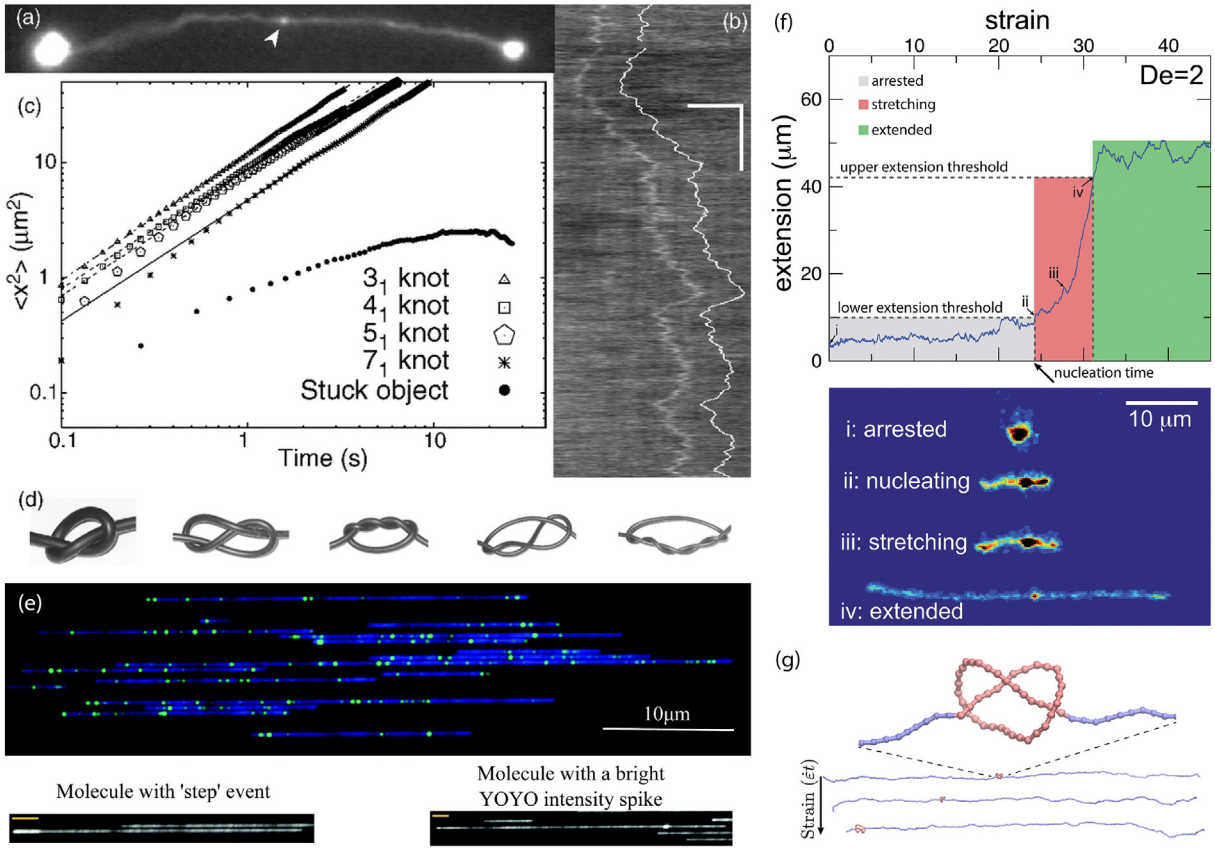

Fig. 1. Visualization of DNA knots. (a) Knotted DNA appears as a diffraction-limited contour between two beads, with an increase in fluorescence at the knot (arrow). (b) A diffusive trace indicating a knot's trajectory. Scale bars, 5 μm (horizontal) and 5 s (vertical); scale of (a) is the same as the horizontal scale of (b). (c) Mean squared distance of knot traveled as a function of time *t*. (d) Topologies of single open knots, from left to right: 3_1, 4_1, 5_1, 5_2, and 7_1. (e) Two-color imaging of DNA in a nanochannel array, with barcodes shown in green and YOYO-1 in blue. Examples of topological events are shown below, specifically a fold at a leading edge fold (left) and high intensity event (right). (f) Stages of stretching self-entangled DNA. (g) Trefoil knots along a bead-rod polymer chain.

Reprinted (a)–(d) with permission from X. R. Bao, H. J. Lee, and S. R. Quake, *Physical Review Letters*, **91**, 265,506. Copyright (2003) by the American Physical Society. Adapted (e) from Ref. 26 with permission of The Royal Society of Chemistry under CC BY 3.0. Reproduced (f) from Ref. 37•• with permission of The Royal Society of Chemistry under CC BY-NC 3.0. Reprinted (g) with permission from C. B. Renner and P. S. Doyle, *ACS Macro Letters*, **3**(10), 963–967. Copyright (2014) American Chemical Society.

knotting and unknotting dynamics. These topics have motivated detailed computational investigations of knots on open chains. For tight, localized knots, such as those generated by optical tweezers, loop closure and subsequent knot classification are relatively straightforward. Robust and efficient closure of complex knots generated in silico, however, poses a non-trivial problem. To address this challenge, Tubiana et al. developed a minimally interfering closure method to characterize entangled knots along an open polymer [21•]. This method enabled many of the recent computational studies on single knotted polymers in the past half-decade, several of which are highlighted in this section.

2.1. Knots in semiflexible polymers: considerations for knotted DNA

It is well known that double stranded DNA molecules are semiflexible polymers and exhibit notably different behaviors in comparison to truly flexible polymers [22]. Chain flexibility is often defined by the persistence length ℓ_p, which can be viewed as the distance along a polymer backbone over which local tangent vectors become uncorrelated. The bare, non-electrostatic persistence length of double stranded DNA is $\ell_p \cong 50$ nm, in contrast to $\ell_p < 1$ nm for many synthetic organic polymers. Knots are intrinsically bent and twisted, and the resulting knotted structures will be intimately affected by molecular properties such as chain thickness and flexibility. From this view, we begin our discussion of knots in DNA with a brief evaluation of the role of semiflexibility on knot properties and dynamics.

Grosberg and Rabin predicted that semiflexible wormlike chains form metastable knots, which spontaneously adopt a well-defined size, diffuse along a polymer, and eventually release from the chain end [23]. The knot contour is described as occupying a confining tube that has (itself) been pulled into a tight knot. Knot formation results in a free energy penalty with competing contributions from the bending energy and confining energy of the polymer, which lead to knot swelling and contracting, respectively.

Doyle and coworkers studied metastable knots with Monte Carlo simulations of long, linear semiflexible polymers [24•]. This work determined the probability and size distributions of trefoil knots along chains of zero thickness with contour length $L_c > 400\ \ell_p$. With these dimensions, roughly one quarter of the simulated polymers formed trefoil knots, with a peak knot size of 12 ℓ_p. The most probable knot size was also shown to be independent of L_c, in agreement with the Grosberg–Rabin predictions. Conversion of knotting probabilities to a potential of mean force resulted in a local minimum at the most probable knot size, whereas the global minimum corresponds to the unknotted state. The potential well was relatively broad, such that chains accommodate large knots with highly variable size; the depth of the potential well (~6 kT) indicates that unknotting events may be more likely to occur via knot diffusion than swelling of the entire molecule.

More realistic polymers were also simulated by modifying the Grosberg–Rabin theory to accommodate nonzero chain width [24•]. As the polymer thickness increased, knotting probability monotonically decreased, the potential well became more shallow, and the most probable knot size increased. These trends reveal the interplay between length scales in real, semiflexible polymers. With consideration of appropriate scaling relations, it is possible that the understanding gained from studies of knotted DNA can be applied to polymers of varying flexibility.

2.2. Dynamics of knotted DNA polymers in nanoconfinement

Advances in DNA nanotechnology have motivated recent investigations of knotting in polynucleotides, from preventing knot formation during genetic barcoding [25••] to determining viral packaging mechanisms [26]. DNA knots are enhanced by spatial confinement, whether by a viral capsid, intracellular environment, or nanofluidic device. Under confinement, DNA molecules may be more prone to forming loops, internal folds, and self-entanglements.

Nanoconfinement geometries are defined by the number of dimensions with nanoscale features, such that 1D, 2D, and 3D confinement correspond to slits, channels, and cavities, respectively. A polymer is considered confined when the nanofeature dimension d is smaller than a molecule's radius of gyration R_g, such that $d < R_g$. In slits and channels, two primary regimes describe the strength of confinement: weaker de Gennes confinement ($\ell_p \ll d < R_g$) and stronger Odijk confinement ($\ell_p \approx d$).

Knotting behavior differs in the de Gennes and Odijk regimes, as well as in the transition region between these two regimes. Micheletti, Marenduzzo, Orlandini, and coworkers have generated a large body of computational work [26–31] that explores confinement in both regimes and the transition region. Specifically, they applied numerical methods and simulations to characterize the equilibrium and dynamic behavior of DNA confined in spheres [26], tubes [27,29••–31], and slits [28,31]. In these studies, d ranged from 40 nm to 1 μm and DNA contour lengths L_c ranged from 1.2–4.8 μm, corresponding to 24–96 persistence lengths or 3.5–14.0 kilobase pairs (kbp) of unstained DNA.

Monte Carlo simulations collectively revealed that the probability of knot formation and resulting knot topologies depend largely on d, L_c, and the confining geometry [26–28,31]. The physical underpinnings of these trends were explored by applying Brownian dynamics (BD) simulations to observe time-dependent unknotting and knotting events along DNA strands in nanochannels [29••,30••].

The probability of finding a knot along an equilibrium polymer conformation increased with the number of confining dimensions, such that the most knots were detected in spherical confinement, followed by channel-like and slit-like confinements [26–28,31]. Overall, single polymers formed more complex knot topologies in channels compared to polymers in slits: in cases of maximum knotting ($L_c = 4.8$ μm, $d =$ 70 nm), simple trefoil knots (3_1) accounted for ~65% of the knots in slits but only ~50% of knots formed in channels [31].

Both nanoslit and nanochannel confinement resulted in non-monotonic knotting probabilities with respect to d [27,28,31]. Starting from wide channels and slits ($d = 1.0$ μm), the probability of knotting gradually increased as a polymer became more confined, eventually reaching a maximum and sharply decreasing upon approaching strong confinement ($d < 75$ nm). BD simulations revealed that major knotting and unknotting events occurred when polymer ends had atypically large backfolds [29••]. Polymers under very strong confinement are known to minimize entropy by elongation; this spontaneous extension hinders backfolding and looping events, thereby resulting in fewer knotting events in narrower channels. Moreover, knots in strong confinement generally form at shallower depths along the polymer chain, persist for shorter residence times, and adopt simpler topological conformations compared to knots in deeper channels. Analysis of dynamic transitions between various knot topologies revealed successive knotting events to form higher order knots (e.g. 5_1 knot topologies are only accessible by multiple passes of a strand through a loop). In this way, complex knots rarely form in the strongest confinement conditions, even if an existing knot persists for an extended period.

Perhaps not surprisingly, it was found that the probability of encountering a knot increases with increasing L_c, differing by an order of magnitude between $L_c = 1.2$ and 4.8 μm [31]. Longer polymers also accommodate more complex knot topologies. In a BD study of knots in a strongly confined tube ($d = 56$ nm) [30••], the average knot size increased slightly with L_c, but with a weaker dependence in comparison to unconfined polymers. Here, the most probable knot size was relatively constant across L_c, agreeing with the Grosberg–Rabin theory and indicating that test chains were not prohibitively short for studying knotting dynamics. Interestingly, increases in L_c resulted in longer average knot residence times (τ_{knot}) while having negligible effects on the duration of unknotted chain events (τ_{unknot}). The disconnect between τ_{unknot} and L_c was elucidated by detailed analysis of spontaneous knot

formation, which revealed that tying and untying events occurred exclusively near the ends of DNA chains in strong confinement. In this way, the frequency of knotting and unknotting events is independent of length. This finding was supported by the probability distribution of short-lived knots, which was also independent of L_c. Dynamic trajectories indicate the longer *average* values of τ_{knot} are dominated by rare events in which knots on longer polymers travel deep into the chain and achieve long dwell times.

Overall, these recent computational studies have provided additional insight into the mechanisms of knotting in confinement. One major shortcoming, however, is the apparent disconnect between simulation parameters and common experimental approaches. Fabricated nanofluidic channels are typically rectangular in dimensional cross-section and may exhibit interactions and soft repulsions with DNA, which may differ from hard, confining cylindrical tubes commonly used in simulations. Moreover, the polymers studied in these simulations generally have much smaller contour lengths compared to DNA commonly used in single polymer experiments, for example lambda phage DNA (λ-DNA, 48.5 kbp, 16 μm unstained or 21.1 μm under typical fluorescent labeling with YOYO-1) [32].

In order to resolve these apparent differences between experiments and simulations, Doyle and coworkers studied metastable knot size in rectangular nanochannels [33]. Monte Carlo simulations of relatively long polymers ($L_c = 400\ell_p$, ~20 μm for dsDNA) in channels with square cross-sections reproduced non-monotonic knot sizes with respect to confinement strength. Rigorous comparison to the Grosberg–Rabin theory captured trends between the most probable knot size, chain width, and confining dimension. Even though these simulations mirrored realistic experimental conditions, the feature sizes encountered in DNA knots remain difficult, if not impossible, to resolve using diffraction-limited fluorescence imaging techniques.

Small feature sizes encountered in polymeric knots is further evident in experimental observations of DNA topology in nanochannel confinement [25••]. In single molecule genetic barcoding, topological events can lead to misreads, thereby decreasing data quality. To understand the nature of these events, single molecules of genomic DNA from *Escherichia coli* were loaded onto a nanochannel array, and molecules were driven by electrophoresis and pre-stretched in an obstacle array to promote uniform loading into nanochannels. Reference labels were introduced to generate unique barcode labels for DNA, and DNA was lightly stained with YOYO-1 to detect topological anomalies (Fig. 1e). In these experiments, measurements consist of dual-color snapshots, and the absence of temporal data is compensated by high throughput, such that this study included 189,153 DNA molecules.

Despite pre-stretching, topological events were detected on 7% of the DNA molecules [25••]. Over half of these events occur at the leading edge of a DNA molecule driven into a nanochannel. The remaining events were evenly distributed along the length of a molecule, with a slight increase near the trailing edge. The increase at trailing edges likely corresponds to spontaneous knotting and unknotting events as described by Brownian dynamics simulations [30••]. Topological event intensities are normalized to adjacent regions of DNA, and relative fluorescence emission intensities are mapped into probability distributions. Events at leading edges exhibit relative fluorescence intensities of ~2, which corresponds to a polymer folding event within a nanochannel. Interestingly, other events show a ~3.3× average increase in intensity relative to adjacent regions of similar size. This increase could correspond to DNA backfolding within a channel or formation of a trefoil knot. These events also skew toward higher intensities, which suggests complex knot formation; unfortunately, rigorous classification of individual topological events is generally not possible using diffraction-limited imaging. Although the initial goal of this work was to study the impact of topology on genome mapping, it is possible that this experimental platform could be leveraged to compare knotting topologies to computational results.

2.3. Mechanical response of self-entangled DNA polymers

Knots in confined polymers arise due to specialized scenarios, in which spontaneous knot formation is a result of the interplay between backfolds, loops, and entropic-driven extension. Aside from confined polymers, how does a knot behave in non-confined systems? As mentioned in Section 1, this problem has been studied using optical tweezing of dual-tethered DNA molecules [20•]; however, a drawback to this approach was the low throughput of knot formation: Bao et al. note that of 100 successful knotting events, only one third provided useful data.

Doyle and coworkers reported a technique to form knotted DNA in dilute solutions by applying a uniform electric field to single DNA molecules [34•]. It was observed that strong electric fields result in isotropically compressed DNA coils, which presumably promotes the generation of a self-entangled polymer. Following the removal of the electric field, single DNA molecules are observed to relax back to non-compressed coils. Relaxation dynamics were categorized into two distinct re-expansion behaviors according to changes in R_g. In the first category, R_g smoothly and continuously returned to the expected equilibrium average; these cases were characterized as unentangled coils. In the second category, expansion was characterized by a three-stage process: (1) an initial arrested state with minimal conformational fluctuations, (2) a nucleation event leading to a second arrested state with a visible compact core, and (3) rapid vanishing of the core and recovery of the equilibrium R_g. The stage-wise relaxation mechanism is attributed to the formation of self-entanglements during compression. Coupling electrohydrodynamic compression with low molecular weight polymer additives enables quick and reliable generation of self-entangled molecules [35].

The impact of self-entanglements on polymers was further probed using single molecule stretching experiments (Fig. 1f) [36••] and simulations (Fig. 1g) [37••]. A planar elongational electric field was generated in a microfluidic cross-slot device, according to Eq. 1, where v_x and v_y are velocity in the x and y directions, and $\dot{\varepsilon}$ is the strain rate of the field.

$$v_x = \dot{\varepsilon}x; v_y = -\dot{\varepsilon}y \tag{1}$$

The strength of the deformation rate can be characterized by the Weissenberg number, $Wi = \tau\dot{\varepsilon}_1$, where τ_1 is the longest polymer relaxation time. Linear polymers are known to undergo a coil-to-stretch transition (CST) at $Wi \approx 0.5$ in elongational fields. In this way, DNA polymers in initially relaxed or initially self-entangled conformations were transiently stretched (Fig. 2a–d) [36••].

Across a wide range of dimensionless flow rates ($1 < Wi < 5$), self-entangled polymers stretched over drastically longer timescales compared to unentangled polymers (Fig. 2e–f). Progressive, stage-wise dynamics were observed, in analogy to the expansion of compressed polymers described before. Unentangled polymer stretching trajectories included a near-immediate transient stretching process followed by steady-state extension, in agreement with prior studies of stretching dynamics [14]. Self-entangled polymer stretching trajectories were characterized in a three-stage process (Fig. 1f): (1) an initial metastable arrested state, (2) a nucleation event followed by transient stretching, and (3) steady-state extension.

Decomposition of traces as a function of stage revealed 50% slower transient stretching of self-entangled molecules compared to unentangled molecules. Self-entangled DNA also contained bright spots that localized and persisted through the stretching trajectories, indicative of knot formation. Moreover, knotted polymers reached shorter steady-state extensions compared to unentangled polymers; this difference was characterized as the excess knot length $\langle L_{knot}\rangle$ due to the contour contained in self-entanglements. $\langle L_{knot}\rangle$ decreased with increasing Wi, consistent with the tightening of a knot under tension.

The single molecule dynamics of self-entangled polymers were qualitatively described using a simple, non-Brownian dumbbell model [36••]. Here, a polymer molecule's contour is divided into free and

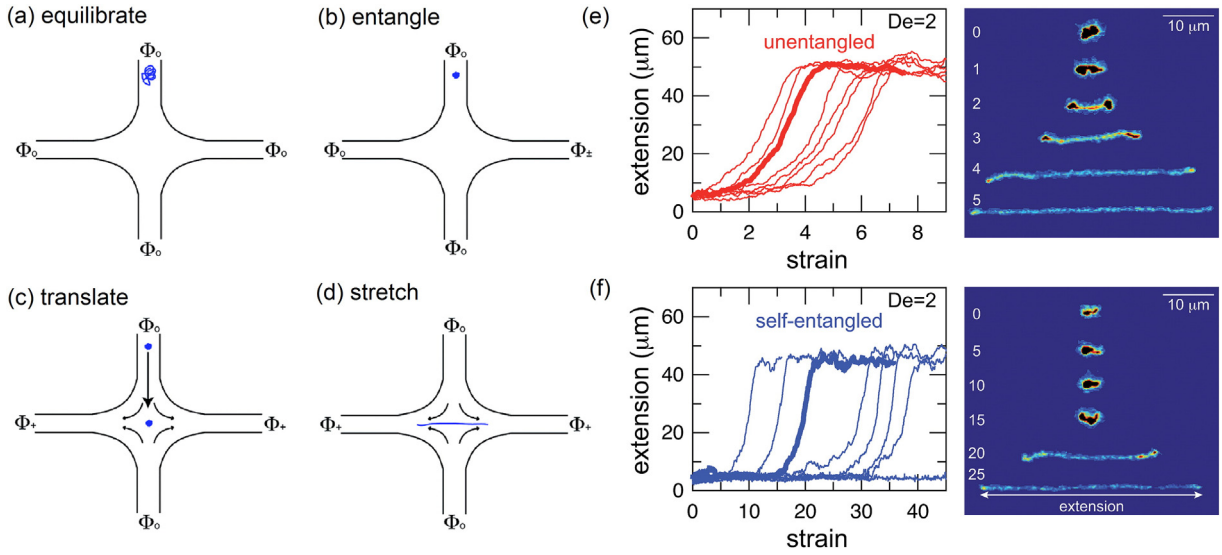

Fig. 2. Stretching unentangled and self-entangled DNA. Schematic of experiment, single molecule trajectories, and single molecule snapshots of the stretching process are shown for self-entangled DNA molecules. (a) A molecule is equilibrated under no field before (b) self-entanglement via electrohydrodynamic compression, (c) translation to the center of the cross-slot device, and (d) stretch in planar extension. Unentangled molecules are translated, equilibrated, and then stretched. Extension versus strain trajectories for (e) unentangled and (f) self-entangled molecules (note different x-axis scales). Bold trajectories correspond to single molecule snapshots, in which the accumulated strains are displayed in white. Adapted from Ref. 37•• with permission of The Royal Society of Chemistry under CC BY-NC 3.0.

entangled portions, L_f and L_e. The deformation field acts only upon L_f, and a transient Weissenberg number accounts for the changing relaxation time of the free contour according to Eq. 2.

$$Wi_f = Wi\left(\frac{L_f}{L_c}\right)^2 \tag{2}$$

For fixed $\dot{\varepsilon}$, Wi is constant, but Wi_f grows as the polymer changes from its initial entangled state ($L_e \gg L_f$) to progressive freeing of ends ($\langle L_{knot}\rangle \sim L_e \ll L_f$). The details of the model are based on transport mechanisms of the polymer contour, which are proposed as diffusive release of entanglements and convective transport of ends (i.e., pulling ends out of an entangled region). Despite the simplicity of this model, a rough estimate of knot friction matched optical tweezer measurements of friction in complex knots [20•].

Although the dynamics of specific knot topologies cannot be probed after electrohydrodynamic collapse, simulations again provide a deeper look into the impact of topology on single polymer dynamics. Renner and Doyle applied BD simulations to study knots on short DNA molecules (3 μm) in elongational flow [37••]. Specifically, knot position was tracked while applying extensional flow on an initially knotted polymer (Fig. 1g). Under a range of dimensionless flow strengths ($1.6 < Wi < 24$), 1D motion of the knots was shown to be strongly dependent on knot topology and nearly independent of tension.

Knot topology was found to impact both diffusive and convective regimes of motion, with particularly interesting dynamics arising in the convection-dominated regime. All knot positions lagged the deformation of the applied flow, and knot topology dictated the degree of lag. In fact, torus knots exhibited much faster convection than non-torus knots, and conformations of torus knots revealed a "corkscrew" translation mechanism of global, sustained rotations along the polymer chain. Conversely, all non-torus knots had similar rates of convection, despite drastically differing sizes. This trend suggests topological self-interference, where convection rates are related to the rate of self-reptation of a knot along a polymer.

The majority of recent work has focused on stretching dynamics of self-entangled polymers in strong flows $Wi > 1$, but we anticipate interesting dynamics at lower field strengths, particularly in the vicinity of the CST. Several key questions remain to be addressed. Does the presence of a self-entanglement shift the CST? Would weak deformation allow for unknotting events, such as the diffusive expansion of compressed coils? Finally, studies of self-entanglements introduced by electrohydrodynamic compression would immensely benefit from a method to elucidate knot topology.

3. Ring polymers

Ring polymers exhibit remarkably different dynamics compared to linear chains and are a topic of current and growing interest in the field. The introduction of a single topological constraint via ring closure drastically changes the dynamic response of circular polymers in flow [7,38–40•]. Moreover, the rheological behavior of melts of circular polymers is highly sensitive to linear contaminants, leading to conflicting experimental reports from bulk-scale techniques [7,38]. For these reasons, several open questions remain regarding the physical mechanisms in these systems. Single molecule techniques are uniquely suited to study these effects by direct visualization of polymer topology and conformation [39••–48•].

Several years ago, Smith and coworkers developed a collection of circular DNA molecules spanning two orders of magnitude in molecular weight (2.7–289 kbp) that can be propagated in bacterial cell hosts [49]. Standard molecular cloning techniques enable reasonable yields from laboratory-scale bacterial cultures and control over linear, relaxed circular, and supercoiled circular topologies during sample preparation. As a result, recent and ongoing work is aimed at probing the impact of polymer topology on single molecule diffusion [41–48•], relaxation [39••,48•,50], and elongation [39••,40•,43••,44].

In addition to single polymer dynamics, circular polymers are rich in topological phenomena. In closed loops, knots have rigorous definitions [17]. For closed circular DNA, the double helical backbone can accommodate twists and writhe, which can lead to supercoiled structures [10,11]. While several open questions remain in these systems, this section of our review focuses on the use of circular DNA as a model polymer in dilute, entangled, and topologically heterogeneous polymer solutions.

3.1. Dynamics of unentangled ring polymers

3.1.1. Diffusion in free solution

Early single molecule studies of circular DNA confirmed the topological independence of power-law scaling behavior for center-of-mass polymer diffusion [41]. The diffusion coefficient D follows an inverse power-law scaling with molecular weight, such that $D \sim R_g^{-1} \sim L_c^{-\nu}$, where the scaling exponent $\nu = 0.5$ in theta solvents and $\nu \cong 0.588$ for good solvents [2]. Diffusion measurements obtained for multiple molecular weight samples spanning 6–290 kbp resulted in $\nu_L = 0.571 \pm 0.014$, $\nu_C = 0.589 \pm 0.018$, and $\nu_S = 0.571 \pm 0.057$ for linear, relaxed circular, and supercoiled circular DNA, respectively.

Despite the near-identical molecular weight scaling behavior of topologically distinct polymers, circular polymers diffuse more quickly than linear polymers of identical length ($D_{circular}$ / $D_{linear} \cong 1.32$). Qualitatively, faster diffusion of rings is attributed to the constraint of ring closure, which decreases a polymer's mean square end-to-end distance. Quantitatively, the exact value of this ratio is still unclear, as a recent study by Habuchi and coworkers reported measurements indicating a ratio of $D_{circular}/D_{linear} \cong 1.1$ [42•]. Current models predict ratios ranging from 1.1–1.45, exhibiting sensitivity to solvent conditions, molecular weight, hydrodynamic interactions (HI), and excluded volume (EV) effects [41].

The study by Habuchi and coworkers revisited single polymer diffusion primarily to verify a new method of image analysis called cumulative area (CA) tracking [42•]. This method tracks the cumulative area occupied by a molecule over time and capitalizes on the connection between temporal fluctuations and molecular size, diffusion, and chain conformation. CA tracking resulted in reportedly precise measurements of diffusion coefficients and holds potential to clarify discrepancies in measured ratios of $D_{circular}/D_{linear}$.

3.1.2. Enhanced polymer mobility in crowded solutions

In cells, DNA exists in a crowded microenvironment due to surrounding macromolecules, thereby prohibiting DNA molecules from freely diffusing in dilute solution as described in Section 3.1.1. Macromolecular crowding agents drive biological functions while varying in size, shape, and chemistry; for these reasons, understanding DNA dynamics in the context of the cellular environment remains a challenge across several scientific disciplines [51].

Robertson-Anderson and coworkers have begun to map the topological aspects of this problem, specifically by measuring and comparing the mobility of linear and circular DNA in crowded solutions [43••,44]. Dextran, an inert branched polysaccharide, is a crowding agent commonly used to mimic intracellular proteins [51]. It was observed that the DNA diffusion coefficient D decreased with increasing dextran size and volume fraction Φ; however, crowder-induced decreases in mobility were independent of DNA length *and* topology above a critical dextran volume fraction Φ_C. As expected, dextran increased solution viscosities η; however, DNA molecules universally diffused more quickly than predicted by the Stokes–Einstein relation ($D \sim \eta^{-1}$).

Enhanced mobility in dextran solutions was attributed to crowder-induced conformational changes. Linear DNA adopted elongated conformations rather than random coils, thereby maximizing crowder volume and the overall system entropy despite the fact that the linear polymer chain enters a lower entropic state [44]. Although isotropic compaction would further enhance entropic volume effects, it was not observed in these experiments due to the entropic cost of charge repulsion at physiological salt conditions. Circular DNA molecules adopted compacted conformations while exhibiting the same mobility enhancement in crowded solutions as linear DNA [43••]. In contrast to linear DNA, elongated circular DNA conformations would be more energetically costly due to close alignment of two negatively charged strands and significant bending energy at the folded "ends."

Interestingly, both linear and circular DNA molecules "breathe" between conformational states, as characterized by the time and length scales associated with conformational fluctuations [43••]. In dilute cases, ring polymer fluctuations took place over ~1.3× shorter time and length scales compared to linear polymers, corresponding to ~1.3× faster diffusion of ring polymers [41]. In the presence of crowding agents, the fluctuations approached a topology-independent timescale above ~2.5Φ_C. Topology-independent fluctuation relaxation times and length scales were coupled, wherein fluctuations normalized by R_{max} remained relatively constant with increasing Φ. In this way, changing time scales due to crowding were coupled with changing step sizes of a DNA molecule's random walk, in turn enhancing mobility.

3.1.3. Ring polymers in non-equilibrium flows

As described in Section 2.3, studies of self-entangled polymers in extensional flow clearly demonstrate the impact of topology on single polymer molecules in non-equilibrium flows. Recent work in this area has focused on the dynamics of circular and linear DNA polymers in planar extensional flow [39••,40•]. As described by Eq. 1 (Section 2.3), a planar extensional field is characterized by a principal axis of compression and an orthogonal axis of extension. Extensional flows are generally considered strong flows, such that polymers can be highly stretched and oriented. Here, planar extensional flow was generated using pressure-driven flow in a microfluidic cross-slot device, and single polymers were confined for extended periods using a hydrodynamic trap [52,53].

Using this approach, single polymer relaxation and stretching dynamics were studied in extensional flow. The longest relaxation time τ_1 of single polymer molecules was measured as a function of molecular weight, specifically comparing 25, 45, and 114.8 kbp circular DNA [39••]. Here, a molecule is stretched to ~70% of its effective contour length, such that $L_{eff} = L_c$ for linear DNA and $L_{eff} = L_c/2$ for circular DNA to account for connectivity of a ring polymer. Upon cessation of flow, the time-dependent maximum projected polymer extension $x(t)$ is fit to:

$$\left(\frac{\langle x(t)\rangle}{L_c}\right)^2 = A\exp\left(\frac{-t}{\tau_1}\right) + B \tag{3}$$

where A and B are fitting constants. The fit is performed over the linear entropic force regime where $\langle x(t)\rangle/L_{eff} < 0.3$, except in the case of 25 kbp circular DNA, where the fit is performed over $\langle x(t)\rangle/L_{eff} < 0.5$ to account for imaging resolution over a shorter effective length [40•].

Ring polymers relaxed more rapidly than linear chains of the same molecular weight; this difference is attributed to an altered relaxation mode structure in the absence of free ends [40•]. Power law scaling behavior was also observed for both circular and linear polymer relaxation. Zimm scaling predicts $\tau_1 \sim L_c^{3\nu}$, such that $3\nu = 1.5$–1.76 for solvent quality varying between theta and good solvents [2]. Scaling for linear ($3\nu_L = 1.71 \pm 0.05$) and ring ($3\nu_R = 1.58 \pm 0.10$) polymers were within this predicted range, and the smaller exponent for ring polymers suggests a decrease in EV effects, perhaps due to the shorter L_{eff} [39••].

Ring polymers also show a coil-to-stretch transition in extensional flow, though the behavior was found to differ from that of linear polymers. Here, the steady-state extension of single ring polymers was studied as a function of Wi, and it was observed that the onset of ring polymer stretch required a higher critical flow strength compared to linear polymers ($Wi_{c,ring} \cong 1.25Wi_{c,linear}$) [39••]. In this way, rings required stronger flows to match the degree of stretch of linear polymers, and rescaling all steady-state extension data by a factor of $Wi_{c,ring}/Wi_{c,linear} \cong 1.25$ superimposed the curves for linear and circular polymer topologies. BD simulations reproduced the shift in $Wi_{c,ring}$ in the presence of HI [40•]. Analysis of specific forces within a ring polymer suggest a strong influence of intramolecular HI for circular polymers, such that parallel strands of the ring exert secondary backflows on each other during stretch (Fig. 3a). The proposed coupling mechanism between HI and polymer topology is further supported by 3D conformations generated by BD simulations, which reveal a stretched "loop"

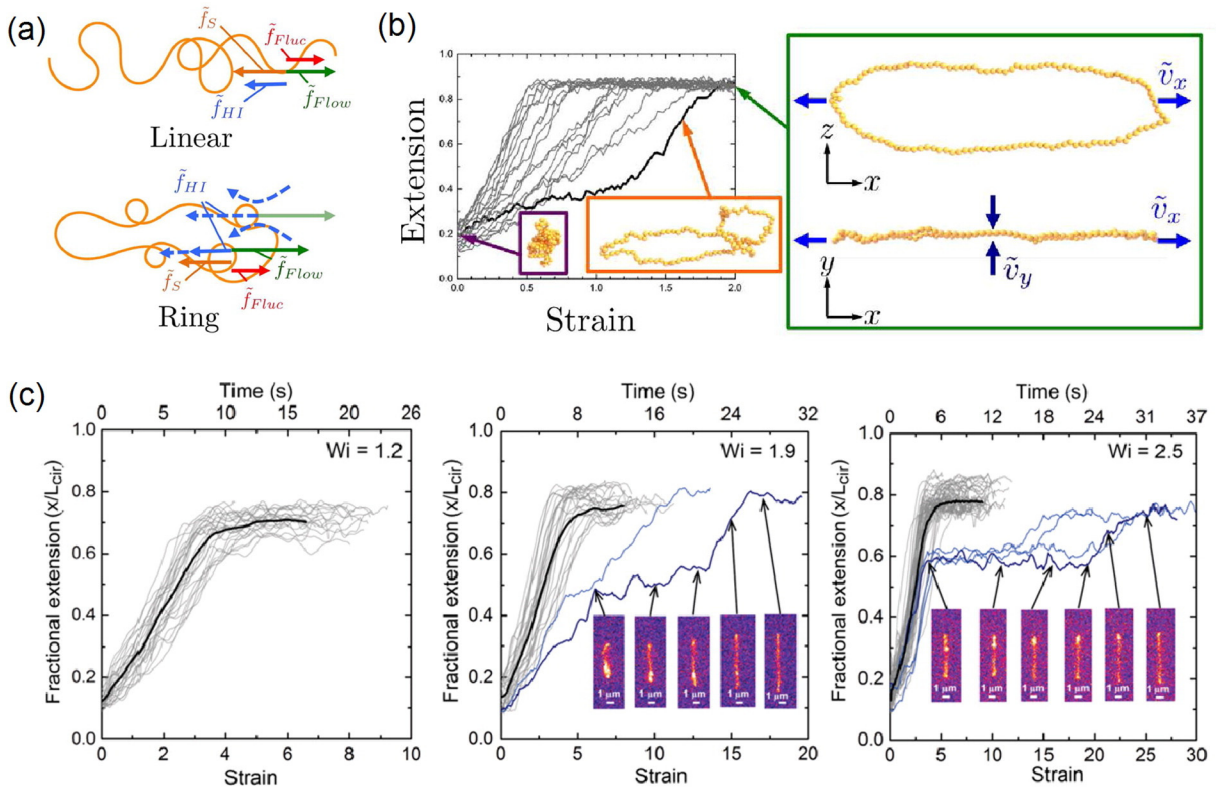

Fig. 3. Stretching of ring polymers in extensional flow. (a) Schematic of the forces on moderately stretched linear and ring polymers. In both cases, the Brownian and entropic spring forces are essentially the same. The ring experiences stronger hydrodynamic forces, where two stretching portions of the ring polymer exert backflows felt by the opposite strand, and a stronger applied fluid flow is required to maintain the same stretch. (b) 3D conformations from Brownian dynamics simulations demonstrating hairpin and looped conformations of transiently stretching ring polymers. Note that loop extension in the *z*-direction is orthogonal to the *xy*-flow plane. (c) Single molecule experimental transient stretch of DNA rings as functions of time and strain ($\varepsilon = \dot{\varepsilon}t$) for $Wi = 1.2$, 1.9, and 2.5. Bold curves represent ensemble averages ($\langle x(t)\rangle/L_{eff}$). Interrupted stretching trajectories are blue, and continuously stretching trajectories are gray. Single molecule images demonstrate the formation and release of transient knotting events.
Adapted (a) and (b) with permission from Hsiao, Schroeder, and Sing, *Macromolecules*, **49**(5), 1961–1971. Copyright (2016) American Chemical Society. Adapted (c) with permission from Li, Hsiao, Brockman, Yates, Robertson-Anderson, Kornfield, San Francisco, Schroeder, and McKenna, *Macromolecules*, **48**(16), 5997–6001. Copyright (2015) American Chemical Society.

conformation wherein rings open into the *z*-direction orthogonal to the planar extensional field (Fig. 3b).

Interestingly, transient dynamics of ring polymers revealed two primary stretching pathways: continuous elongation and interrupted elongation (Fig. 3c) [39••]. These behaviors contrast the spectrum of conformations observed for linear polymers: dumbbell, half-dumbbell, kinked, and folded states. This reduced degree of molecular individualism of circular DNA relative to linear DNA is consistent with the notion that circular molecules have fewer degrees of freedom due to their connectivity. Experimentally, interrupted elongation pathways appeared to form transient knots that hindered stretch until their eventual release. This behavior was reproduced in BD simulations, in which hairpins and loops in the *z*-direction are associated with slow unfolding behaviors (Fig. 3b) [40•].

3.2. Diffusion of entangled ring polymers

A single, linear polymer molecule in an entangled solution or melt is known to move by reptation, wherein polymers diffuse through an effective confining potential or confining tube by a snake-like motion [2,54]. Circular polymers, however, have no ends. Clearly, ring polymers must utilize a fundamentally different mechanism to move and translate in entangled solutions.

In synthetic organic polymer chemistry, the preparation of topologically pure solutions or melts of ring polymers is a challenging problem. Furthermore, trace quantities of linear polymers are known to drastically change the rheological behavior of entangled ring polymers. Even with recent advances in synthesis and purification, bulk measurement techniques lack the molecular resolution needed to fully understand ring polymer mechanisms [7,38]. Enzymatic transformations enable topological control over DNA molecules [41,49], which further emphasizes the suitability of DNA as a suitable system for studying entangled ring polymers. Single molecule studies of ring and linear polymer self-diffusion in topologically pure and heterogeneous (blended) solutions provide direct evidence of new mechanisms for ring polymer motion, in addition to clarifying anomalous behavior of rings in the presence of linear impurities.

Upon demonstrating the facile preparation of topologically pure, entangled DNA solutions, Robertson and Smith thoroughly investigated the impact of topology, molecular weight, and concentration on single polymer diffusion [45••–47••]. Systematic studies of fluorescent tracer molecules entangled in a background matrix probed several topological combinations of linear and circular polymers, as depicted in Fig. 4a using a labeling convention of (tracer-matrix): linear tracer molecules in a matrix of linear (L-L) or circular (L-C) polymers, as well as a circular tracer molecules in a matrix of linear (C-L) or circular (C-C) polymers.

Self-diffusion measurements revealed the greatest overall effect between different matrix polymer topologies (Fig. 4b) [45••,46], where linear or circular tracers in an entangled circular matrix diffused orders of magnitude more quickly than linear or circular tracers in an entangled linear matrix. In unentangled matrices (lower concentration or molecular weight DNA), the effect of topology was negligible and diffusion coefficients of all combinations were maintained within a factor of two. Overall findings for diffusion coefficients in entangled solutions were $D_{C\text{-}C} \gtrsim D_{L\text{-}C} \gg D_{L\text{-}L} \gg D_{C\text{-}L}$, which led to several predictions for the molecular motions of ring polymers: first, linear polymers are capable of pinning or threading through rings, slowing ring diffusion until release of the linear constraint ($D_{C\text{-}L} \ll D_{L\text{-}L}$); second, constraint

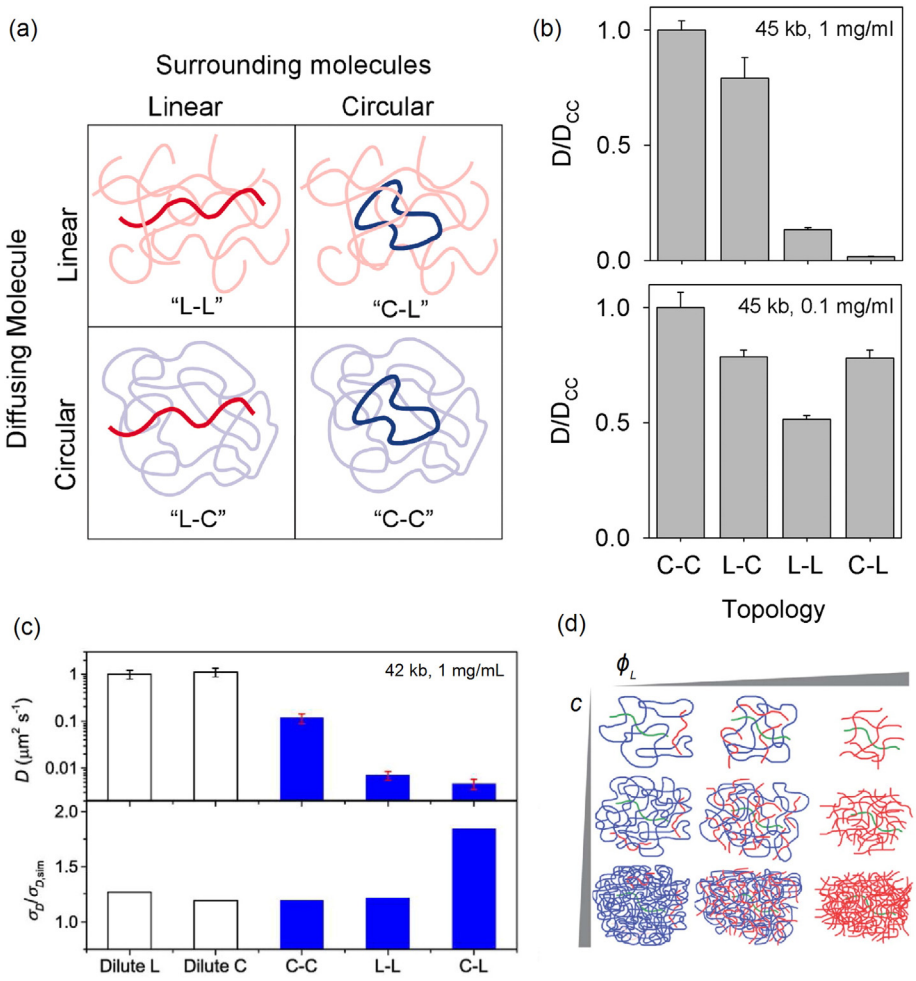

Fig. 4. Single molecule diffusion of circular and linear DNA. (a) Topological combinations of linear or circular tracer molecules (bold) in a background matrix of linear or circular polymers. (b) DNA self-diffusion coefficients as a function of topology in entangled (1 mg/mL, top) and unentangled (0.1 mg/mL, bottom) solutions. (c) DNA self-diffusion coefficients (top) and distributions (bottom) measured by CA tracking. (d) Schematic of the concentration and blend composition parameter space for a linear tracer molecule (green) surrounded by circular and/or linear DNA. The same parameter space is tested using circular tracers.
Adapted (a) and (b) from Robertson and Smith, *Proceedings of the National Academy of Sciences*, **104**(12), 4824–4827. Copyright (2007) National Academy of Sciences, USA. Adapted (c) with permission from Abadi, Serag, and Habuchi, *Macromolecules*, **48**(17), 6263–6271. Copyright (2015) American Chemical Society. Adapted (d) with permission from Ref. 47•• with permission of the Royal Society of Chemistry.

release involving a threaded linear chain is a slower process than reptation in these systems; third, constraint release is negligible in pure ring matrices.

Habuchi and coworkers further explored these predictions by applying CA tracking (Section 3.1.1) to entangled DNA [48•], which enabled simultaneous characterization of molecular motion at various length scales and conformational relaxation times. Molecular motions were used to determine diffusion coefficients of C-C, C-L, and L-L polymer combinations, resulting in the same trends where $D_{C\text{-}C} \gg D_{L\text{-}L} \gg D_{C\text{-}L}$ (Fig. 4c).

Modes of diffusion were determined by comparison of mean CA trajectories to 1D and 2D random motions, which correspond to different molecular models for ring polymers [48•]. 1D random motions indicate reptation or double-folded reptation, whereas 2D random motions suggest a lattice-animal model in which cyclic polymers adopt double-folded linear conformations with multiple loops. Dilute polymers diffused via 2D motion only, as expected for Brownian motion, and all entangled combinations recovered 2D random motion and random walks at long length scales.

Conformational relaxation times were determined by analyzing temporal fluctuations of the area occupied by a molecule, such that autocorrelation functions of molecular fluctuations were fit to a single exponential decay. Pure entangled ring polymers (C-C) exhibited similar conformational relaxation times in comparison to dilute rings, despite slower diffusion. At short length scales, diffusive motions followed neither 1D nor 2D random motions, suggesting a different mechanism for ring polymer motion than predicted by either reptation or lattice animal models. Habuchi and coworkers suggest *mutual relaxation* of ring polymers, where intermolecular constraints are negligible because rings do not thread each other. All data acquired for pure entangled linear polymers (L-L) agreed with reptation motion, including 1D diffusive behavior at short length scales. Surprisingly, only 2D motion was observed for C-L systems, such that cyclic molecules exhibited isotropic motion in linear polymer backgrounds. Heterogeneity in diffusion coefficients revealed larger distributions in $D_{C\text{-}L}$ compared to other cases, suggesting heterogeneous molecular-level interactions, such as variable threading of linear polymers through a tracer ring polymer [48•].

An investigation of blends of linear and circular DNA by Robertson-Anderson and coworkers supports the notion of variable threading [47••]. Self-diffusion coefficients of linear and circular tracers were measured at varying concentrations below, near, and above the entanglement concentration in blends of linear and ring polymers, as depicted for linear tracers in Fig. 4d. Blend fractions were incremented from pure circular ($\phi_C = 1.0$, $\phi_L = 0$) to pure linear ($\phi_L = 1.0$, $\phi_C = 0$) in steps of 0.1. Diffusion coefficients were independent of blend composition in all unentangled solutions.

Near or above entanglement, ring polymer tracers diffused quickly when $\phi_L = 0$; upon increasing ϕ_L, D_C rapidly decreased by orders of magnitude before slowly and monotonically decreasing. This behavior is consistent with measurements in topologically pure solutions, as well as a minimal constraint model for binary blends of ring and linear polymers [55].

Unexpectedly, D_L responded non-monotonically to changes in blend composition, reaching a minimum near $\phi_C \sim \phi_L \cong 0.5$ [47••]. This behavior was not predicted by the minimal constraint model, rather, slight modifications incorporating the impact of ring threading on linear polymers were required to capture the experimental findings. Briefly, the relaxation times of circular and linear polymers are modeled as functions of blend composition ($\tau_R(\phi_L)$ and $\tau_L(\phi_L)$, respectively), with contributions from the average number of entanglements per molecule in a linear melt and the average number of linear polymers threading a ring [55]. Numerical evaluation of this model uncovered criteria for non-monotonic behavior, such that a crossover must occur between D_C and D_L [47••].

Intuitively, the trends in diffusion coefficients can be explained by considering the transition between pure circular and linear solutions. At $\phi_L \approx 0$, a small fraction of rings are threaded by linear polymers while most rings diffuse freely. As ϕ_L increases, both the fraction of threaded rings and number of threads per ring increase, monotonically increasing τ_R until threading events plateau as ϕ_L approaches unity. Considering the opposite transition for linear polymers, when $\phi_L = 1$, all polymers have the same relaxation time τ_L. When one background linear polymer is replaced with a ring polymer, the solution has exchanged a somewhat mobile constraint with a less mobile, threaded ring polymer, and $\tau_L(\phi_L)$ increases. As more constraints are replaced (ϕ_L decreases from 1), $\tau_R(\phi_L)$ concurrently decreases, reaching some point at which $\tau_R(\phi_L) = \tau_L(\phi_L)$. As ϕ_L decreases from this point, the exchange between constraining molecules introduces more mobile rings, so $\tau_L(\phi_L)$ decreases. This competition between structure and dynamics results in a maximum in $\tau_L(\phi_L)$ or a minimum in $D_L(\phi_L)$, and supports proposed mechanisms of variable threading between linear and circular polymers in topologically heterogeneous mixtures.

Based on these studies, it is clear that a simple change in polymer topology (ring closure) leads to a wealth of interesting and unexpected dynamic behavior at the single molecule level. Moving forward, additional studies focusing on the nonequilibrium dynamics of rings and topologically complex polymers in entangled solutions will undoubtedly reveal new physics.

4. Branched DNA polymers

Connectivity in polymer chains can be considered in terms of molecular branching or chemical or physical networks [3,5•,6•,8,54,56•]. Networks are formed by chemical or physical crosslinks, which impart topological constraints and elasticity in gels, plastics, and rubbers. Branched polymers are defined as having secondary polymer chains linked to a primary backbone, resulting in a variety of polymer architectures such as star, H-shaped, pom-pom, and comb-shaped polymers.

The molecular properties of branched polymers can be described by a wide parameter space, including chemical structure, backbone molecular weight, branch molecular weight, and branching density. From this view, branched polymers can exhibit broad chemical versatility, thereby giving rise to potentially dramatic changes in rheological behavior [5•,6•,8,56•]. In an entangled solution of combs or comb polymer melts, branch points are known to substantially slow down the overall relaxation processes within the material, especially for high molecular weight branches. Branching often results in a spectrum of relaxation times related to movement of branches, segments between branches, and the entire molecular backbone [6•]. In this way, chain branching is thought to result in extremely complex behaviors at equilibrium and in response to flow.

Recent single molecule studies of branched polymers have only begun to scratch the surface of these phenomena. Although branched structures naturally form in DNA during replication and recombination, these intermediate states are intrinsically transient and generally not suitable as models for covalently linked branched polymers [57]. In this section, we review two independent approaches for synthesis and single molecule studies of branched DNA polymers.

4.1. Star DNA polymers

The instability of branched junctions in DNA (e.g. the Holliday junction) stems from sequence symmetry around a DNA branch point. Asymmetric sequences can be used to generate artificial, immobilized nucleic acid junctions [57]. This technology enabled structural characterization of DNA junctions [58], inspired the burgeoning field of DNA origami [59], and provided a method to create stable branched DNA polymers [60••].

Archer and coworkers carried out initial studies of branched DNA using single polymer techniques [60••–62]. This early work reported important findings and represents a few of only a handful of investigations on single branched polymers. Here, branched DNA was generated by forming a star core of hybridized oligonucleotides with sticky overhangs complementary to the 5′-overhang of λ-DNA (Fig. 5a). λ-DNA molecules were hybridized to the sticky overhangs and ligated to produce DNA stars. This method was also extended to create pom-pom polymers by connecting two stars with a λ-DNA crossbar.

Conformational dynamics and electrophoretic mobility μ of star DNA polymers were measured in solutions of linear polyacrylamide [60••,61] and polyethylene oxide [62], as well as in agarose and polyacrylamide gels [60••]. In dilute solutions, DNA conformations and μ were independent of topology, such that both star and DNA molecules migrated as random coils [60••,62]. In unentangled, semi-dilute solutions, star DNA exhibited inverted squid-like conformations upon interacting with the surrounding polymers (Fig. 5b). Star DNA arms outstretched in the direction of the electric field, pulling star cores through the solution. Despite major conformational differences between linear and star DNA, μ was relatively insensitive to topology; instead, μ was found to depend on the molecular weight and concentration of the background polymer [62].

DNA architecture was found to play a more significant role on μ in entangled solutions of linear polymer backgrounds [60••,61]. Here, linear DNA oriented and aligned with the electric field, migrating with μ independent of background polymer molecular weight. In contrast, star DNA adopted more drastic versions of the inverted squid-like conformations as cores entangled with polymers in the surrounding solution. Star DNA migrated more slowly as the background polymer molecular weight increased [61]. The most drastic conformational difference between stars and linear polymers occurred in gels. Here, it was observed that large DNA stars simply could not migrate through a fixed surrounding network. When driven toward an interface between a semi-dilute polymer solution and a gel, the core of the DNA star was trapped by the fixed constraints of the gel [60••].

These studies began to reveal the impact of branching on single polymer dynamics, albeit in the context of electrophoresis rather than solution-based fluid flows. Moreover, the hybridization-based synthesis approach was not exceedingly efficient, with Archer and coworkers noting overall yields of 5–10% after purification by gel extraction [60••]. Although hybridized DNA junctions have proven useful for oligonucleotide assembly and DNA origami [59], the two-step process of hybridizing and ligating very large arms to a core of small oligonucleotides is kinetically slow, ultimately prohibiting the widespread use of hybridization-based branched DNA for single polymer dynamics.

4.2. Graft-onto branched DNA polymers

A major challenge in single molecule studies of branched DNA is the synthesis of polymers with precisely controlled architectures with

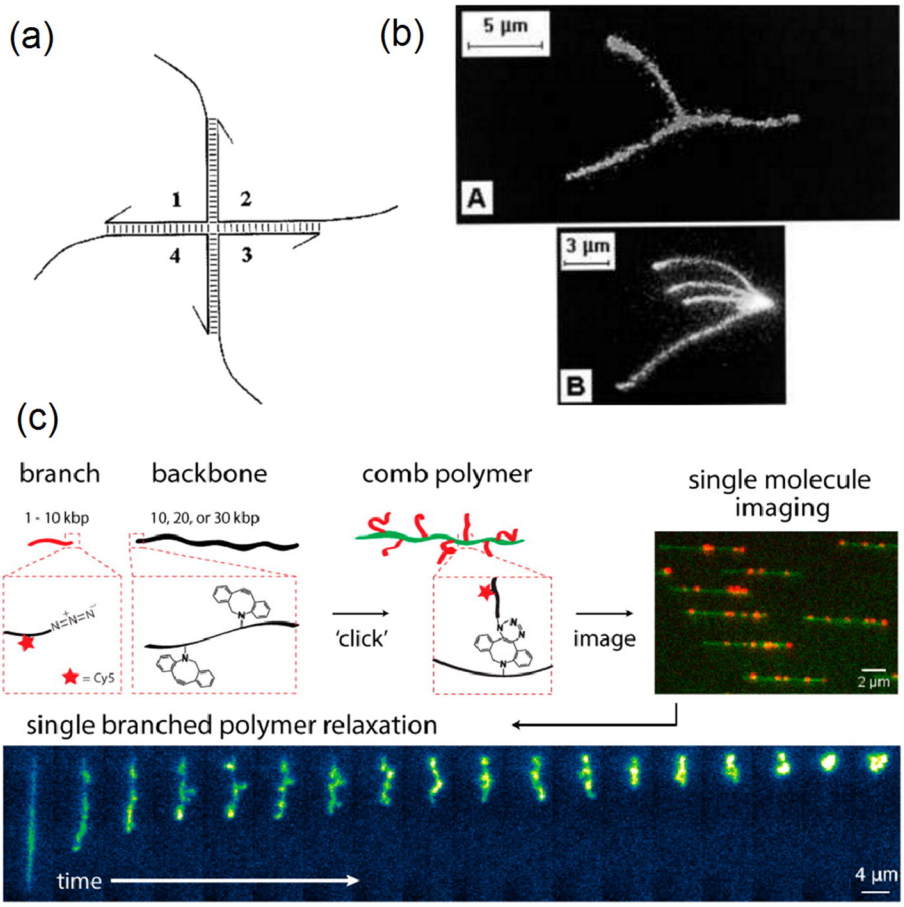

Fig. 5. Synthesis and single molecule imaging of branched DNA. (a) Schematic of a four-arm star core generated by hybridization of oligonucleotides. (b) Large DNA star conformations in concentrated polymer solutions: (top) no applied electric field, (bottom) an electric field is applied with the positive electrode on the left. (c) Synthesis, imaging, and relaxation of graft-onto branched polymers.
Reproduced (a) and (b) from Ref. 60•• with permission of John Wiley and Sons, Inc. Reprinted (c) with permission from D. J. Mai, A. B. Marciel, C. E. Sing, and C. M. Schroeder, *ACS Macro Letters*, **4**(4), 446–452. Copyright (2015) American Chemical Society.

suitable properties for fluorescence imaging. Schroeder and coworkers recently introduced new strategies to address these issues [63•,64••].

Template-directed enzymatic synthesis of DNA was combined with grafting techniques from synthetic organic chemistry (Fig. 5c, left). In this way, DNA building blocks of precise sequence and length were synthesized via polymerase chain reaction (PCR). The inclusion of chemically modified primers and non-natural nucleotides during PCR resulted in the incorporation of internal graft sites, terminal reactive sites, and fluorescent labels. Bioconjugation techniques enabled graft-onto reactions between end-functionalized branches and mid-functionalized backbones, thereby producing stable, branched DNA molecules.

This hybrid enzymatic-synthetic approach was used to synthesize relatively short DNA with precisely defined structures [63•]. Backbone sequences were defined to include graft sites at specified locations, with exact control over the number and spatial arrangement of graft sites incorporated in product polymers during PCR. Topologies included three-arm star, H-shaped, and graft block polymers, with topological possibilities limited only by the template length (50–60 bp in this study). In addition to structurally defined homopolymers, branched copolymers and miktoarm star polymers were also synthesized by grafting poly(ethylene glycol) side branches to DNA templates. Although these polymers generally had low molecular weights that would preclude direct single molecule imaging of molecular conformations, these precision materials hold strong potential for detailed studies of self-assembly and structure–function relationships in branched polymers and block copolymers. Furthermore, grafted DNA oligomers exhibited drastically hindered electrophoretic migration compared to linear polymers, in agreement with electrophoresis of large branched DNA constructs [60••].

The two-step synthetic approach was further extended to generate long branched DNA for single molecule studies of comb polymers [64••]. Here, exact control was maintained over branch length (1–10 kbp) and backbone length (10–30 kbp), with average control over the degree of branching by tuning stoichiometry using a graft-onto approach. As expected, branched DNA products exhibited decreased mobility during gel electrophoresis in comparison to linear DNA.

Inclusion of a chemically modified terminal linker on the backbone enabled specific attachment of branched DNA molecules to a surface, facilitating direct observation of single branched DNA without requiring extensive purification [64••]. In one study, DNA comb polymers consisted of 10–20 kbp backbones and low molecular weight branches (1 kbp) with covalently linked fluorescent labels. Here, molecular branch frequency distributions and polymer end-to-end distances were characterized via simultaneous visualization of polymer branches and backbones (Fig. 5c, right). In regards to branching distributions, single molecule data showed that the number of branches added per backbone was generally less than expected based on simple stoichiometric arguments for incorporation of chemically modified nucleotides and addition of branches during graft-onto reactions. In particular, average branch frequencies ranged from 1.5–10 per backbone, but the theoretical maximum number of graft sites ranged from 100 to 1200. The main source of this disparity likely lies in the discrimination of

non-natural nucleotides against natural nucleotides during PCR, which can likely be overcome by tuning stoichiometry or chemical structure of modified nucleotides.

A separate study directly observed conformational relaxation of larger branched DNA, with 30 kbp backbones and 10 kbp branches (Fig. 5c, bottom) [64••]. Although the stretching dynamics were not investigated in full detail, it was clear that branched DNA exhibited a CST and stretched prior to relaxation upon cessation of flow.

Qualitatively, single molecule videos clearly showed that relaxation processes depend on molecular topology [64••]. At early times in the relaxation process, the backbone and branches exhibited a simultaneous and rapid elastic recoil characterized by a sharp decrease in extension with respect to time. At intermediate times, branched polymers exhibited mixed relaxation dynamics of branches and backbones, such that branches explored various conformational "breathing modes" while the backbone relaxed. The mixing of relaxation modes was likely related to the similar branch and backbone molecular weights in this particular study. At long times, the longest mode of relaxation dominated the process, which corresponds to relaxation of the main polymer backbone. These visual observations empirically suggest that at least two dominant time scales govern the relaxation process, including an intermediate branch relaxation time and the longest backbone relaxation time.

These time scales were quantified in a similar method as described in Section 3.1.3 and Eq. 3, where the time-dependent backbone end-to-end distance was fit to a single exponential decay over the longest relaxation time and length scales, $\langle x(t)\rangle/L_c < 0.3$, or intermediate time and length scales, $0.3 < \langle x(t)\rangle/L_c < 0.5$. The longest relaxation time generally increased with an increasing number of branches, which reflects an increase in friction along the DNA backbone due to pre-relaxed side branches. Intermediate timescales were much more sensitive to the number of branches, as well as branch position. Interestingly, polymers with a single branch behaved similarly to linear polymers on average.

A deeper investigation of branch position revealed a strong dependence of intermediate relaxation time on distance between the branch and surface tether. Branches far from the tether slowed relaxation, whereas branches near the tether resulted in faster overall relaxation processes compared to a linear polymer. Schroeder and coworkers postulated that branches introduce new modes of relaxation between the tether point and the branch end. In the case of a branch far from the tether, the contour length of a branched molecule is effectively increased. In the case of a branch near the tether, the branch relaxes more quickly than the polymer backbone, potentially inducing local hydrodynamic flows that enhance relaxation of the backbone. From a broader perspective, it is important to note that single molecule techniques are quite powerful in revealing these topological effects via direct observation of polymer architecture.

Overall, the vast parameter space of branched polymeric systems remains relatively unexplored by single molecule techniques. The few studies that exist demonstrate the wealth of molecular-scale understanding to be gained by future investigations. Progress toward preparing branched DNA at high yield and purity will enable systematic molecular-scale exploration of the impact of branching on polymer structure, properties, and dynamics. In this way, an improved fundamental understanding of recently observed rheological phenomena will provide insights toward the molecular-scale design of topologically complex polymers.

5. Conclusions

DNA is a remarkably versatile material for single polymer dynamics. In recent years, researchers have leveraged biological, biochemical, and synthetic tools to generate DNA-based polymers with complex molecular topologies. In this review, we summarize recent investigations of knotted, circular, and branched DNA, all of which provide a new fundamental understanding of the interplay between topology and dynamics. This approach can be followed to effectively link experiments, simulations, and theory in single polymer dynamics.

Simulations of knotted and confined DNA elucidate the conditions for knot formation [29••], potentially informing the design of next-generation nanofabricated devices for genetic barcoding [25••]. Self-entangled DNA exhibits new mechanical behavior, forming arrested states and stretching much more slowly in comparison to linear DNA [36••]. Specific knot topology and dynamics are intimately related, and progress toward the resolution and classification of experimentally generated knots will enable the validation of knot models and theories.

Single molecule studies of polymer diffusion in entangled circular and/or linear DNA solutions have revealed the physical mechanisms underlying anomalous behavior in entangled ring solutions and melts. Entangled rings diffuse by non-reptative mechanisms [48•], and threading of circular polymers by linear molecules dramatically reduces the mobility of ring polymers [45••–48•]. In dilute solutions, a coupling between topology and hydrodynamic interactions governs ring polymer dynamics [39,48•], and new experimental techniques raise questions about ring polymer diffusion [42•]. Probing the non-equilibrium dynamics of entangled ring polymer solutions will undoubtedly reveal new physics surrounding topological complexity.

Single molecule studies of branched polymers have only begun to explore the vast parameter space of molecular architecture, but early work already demonstrates strong coupling between molecular topology and dynamics [64••]. Moving forward, future single molecule studies of branched polymer dynamics in dilute, semi-dilute, and entangled solutions will reveal a wealth of information regarding the influence of complex topology on molecular stretching and dynamics.

From a broad perspective, research in the field of single polymer dynamics has uncovered fundamentally new information on polymer physics. Over the last two decades, single polymer studies involving DNA have revealed conformational dynamics at the single molecule level, thereby enabling direct validation and comparisons to predictions of classical scaling theories [2]. Single polymer studies take a step beyond ensemble-level tracer studies in polymer physics by directly revealing phenomena such as molecular individualism, distributions in molecular behavior, and conformational hysteresis in strong flows [32]. However, most advances in the field of single polymer dynamics have largely focused on the dynamics of linear polymers in dilute solution, which represents a fairly narrow parameter space in the field. Importing the powerful methods enabled by single molecule imaging into more complex problems in polymer physics is of paramount importance to the field, including studies of polymers with complex topology in flow, dynamics in entangled solutions, and direct observation of copolymer assembly. Indeed, these topics are areas of active research in the field and promise to deliver exciting results in the near future. To this end, new capabilities in experiments and simulations will extend the reach of single polymer dynamics, and these techniques will be leveraged to study contested assumptions in the field, ranging from the nature of molecular entanglements to polymer crystallization. As one example, single polymer dynamics have already clarified inconsistencies in rheological measurements of circular polymers due to threading of rings by linear chains [7,38,47••]. An additional area of interest includes the proposed relaxation mechanism(s) of entangled polymers (of varying topologies), wherein we lack universal predictive models of branched polymer behavior.

In all areas of topology, single polymer dynamics connect molecular-scale behavior to emergent properties of polymeric materials. DNA has enabled these contributions, given facile preparation of monodisperse samples, topological control, and well-established experimental conditions. New developments in super-resolution imaging and fluorescently labeled synthetic polymers [65] have potential to drive progress in the field beyond DNA. Until then, DNA will continue to serve as

the gold standard for single molecule dynamics of topologically complex polymers.

Acknowledgements

This work was supported by an Illinois Distinguished Fellowship and NSF Graduate Research Fellowship for DJM, as well as the David and Lucille Packard Foundation, NSF CAREER Award CBET-1254340, and the Camille and Henry Dreyfus Foundation for CMS.

References and recommended reading*,**

[1] Grosberg A, Nechaev S. Polymer topology. Polymer characteristics. Berlin, Heidelberg: Springer Berlin Heidelberg; 1993 1–29.
[2] Doi M, Edwards SF. The theory of polymer dynamics. Clarendon Press; 1988.
[3] Flory PJ. Principles of polymer chemistry. Cornell University Press; 1953.
[4] Peurifoy SR, Guzman CX, Braunschweig AB. Topology, assembly, and electronics: three pillars for designing supramolecular polymers with emergent optoelectronic behavior. Polym Chem 2015;6:5529–39.
[5] Daniel WFM, Burdynska J, Vatankhah-Varnoosfaderani M, Matyjaszewski K, Paturej J, Rubinstein M, et al. Solvent-free, supersoft and superelastic bottlebrush melts and networks. Nat Mater 2016;15:183–9 [This study of brush-like polymers demonstrates the impact of molecular topology on the emergent physical properties of polymeric materials.].
[6] van Ruymbeke E, Lee H, Chang T, Nikopoulou A, Hadjichristidis N, Snijkers F, et al. Molecular rheology of branched polymers: decoding and exploring the role of architectural dispersity through a synergy of anionic synthesis, interaction chromatography, rheometry and modeling. Soft Matter 2014;10:4762–77 [This viewpoint on entangled branched polymer melts describes progress toward elucidating the impact of topological impurities in viscoelastic measurements.].
[7] Kapnistos M, Lang M, Vlassopoulos D, Pyckhout-Hintzen W, Richter D, Cho D, et al. Unexpected power-law stress relaxation of entangled ring polymers. Nat Mater 2008;7:997–1002.
[8] Zhou H, Woo J, Cok AM, Wang M, Olsen BD, Johnson JA. Counting primary loops in polymer gels. Proc Natl Acad Sci 2012;109:19119–24.
[9] Lutz J-F, Ouchi M, Liu DR, Sawamoto M. Sequence-controlled polymers. Science 2013;341 [This review article points out progress and challenges in chemical and biological approaches toward synthesizing sequence-controlled macromolecules.].
[10] Bates AD, Maxwell A. DNA topology. Oxford University Press; 2005.
[11] Schoeffler AJ, Berger JM. DNA topoisomerases: harnessing and constraining energy to govern chromosome topology. Q Rev Biophys 2008;41:41–101.
[12] McKinney SA, Declais A-C, Lilley DMJ, Ha T. Structural dynamics of individual Holliday junctions. Nat Struct Mol Biol 2003;10:93–7.
[13] Koster DA, Crut A, Shuman S, Bjornsti M-A, Dekker NH. Cellular strategies for regulating DNA supercoiling: a single-molecule perspective. Cell 2010;142:519–30.
[14] Mai DJ, Brockman C, Schroeder CM. Microfluidic systems for single DNA dynamics. Soft Matter 2012;8:10560–72.
[15] Dorfman KD. DNA electrophoresis in microfabricated devices. Rev Mod Phys 2010; 82:2903–47.
[16] Dai L, Renner CB, Doyle PS. The polymer physics of single DNA confined in nanochannels. Adv Colloid Interface Sci 2016;232:80–100.
[17] Adams CC. The knot book: an elementary introduction to the mathematical theory of knots. Providence, RI: American Mathematical Society; 2004.
[18] Lim NCH, Jackson SE. Molecular knots in biology and chemistry. J Phys Condens Matter 2015;27:354101.
[19] Arai Y, Yasuda R, Akashi K-i, Harada Y, Miyata H, Kinosita K, et al. Tying a molecular knot with optical tweezers. Nature 1999;399:446–8.
[20] Bao XR, Lee HJ, Quake SR. Behavior of complex knots in single DNA molecules. Phys Rev Lett 2003;91:265506 [This work provided the first quantification of knot dynamics on single DNA molecules. The method of knot generation used here enables precise classification of knot topology.].
[21] Tubiana L, Orlandini E, Micheletti C. Probing the entanglement and locating knots in ring polymers: a comparative study of different arc closure schemes. Prog Theor Phys Suppl 2011;191:192–204 [An algorithm for loop closure is presented that enables efficient classification of knot topology in simulations. This algorithm is utilized in the majority of computational studies on knotting dynamics cited throughout this review.].
[22] Latinwo F, Schroeder CM. Model systems for single molecule polymer dynamics. Soft Matter 2011;7:7907–13.
[23] Grosberg AY, Rabin Y. Metastable tight knots in a wormlike polymer. Phys Rev Lett 2007;99:217801.
[24] Dai L, Renner CB, Doyle PS. Metastable tight knots in semiflexible chains. Macromolecules 2014;47:6135–40 [This work computationally validates Grosberg–Rabin theory for knots in semiflexible chains and characterized knotting probabilities in polymers with similar dimensions to DNA.].
[25] Reifenberger JG, Dorfman KD, Cao H. Topological events in single molecules of *E. coli* DNA confined in nanochannels. Analyst 2015;140:4887–94 [This work characterizes topological events occuring along DNA molecules driven into nanochannels. It demonstrates both an experimental platform for studying knotting events in single, nanoconfined DNA molecules and the need for techniques to resolve knot topologies.].
[26] Marenduzzo D, Orlandini E, Stasiak A, Sumners DW, Tubiana L, Micheletti C. DNA–DNA interactions in bacteriophage capsids are responsible for the observed DNA knotting. Proc Natl Acad Sci 2009;106:22269–74.
[27] Micheletti C, Orlandini E. Knotting and metric scaling properties of DNA confined in nano-channels: a Monte Carlo study. Soft Matter 2012;8:10959–68.
[28] Micheletti C, Orlandini E. Numerical study of linear and circular model DNA chains confined in a slit: metric and topological properties. Macromolecules 2012;45: 2113–21.
[29] Micheletti C, Orlandini E. Knotting and unknotting dynamics of DNA strands in nanochannels. ACS Macro Lett 2014;3:876–80 [This study of DNA knot dynamics elucidates the conditions for knot formation as a function of nanochannel size and identified atypically large backfolding events. This work also shows that higher order knots are formed via successive knotting events.].
[30] Antonio S, Enzo O, Cristian M. Knotting dynamics of DNA chains of different length confined in nanochannels. J Phys Condens Matter 2015;27:354102 [This study extends the work of Ref. 31, revealing the independence of knot formation on DNA molecular weight. Larger knot formation probabilities on longer DNA molecules are found to be due to increased knot residence times as knots travel along a chain's contour.].
[31] Orlandini E, Micheletti C. Knotting of linear DNA in nano-slits and nano-channels: a numerical study. J Biol Phys 2013;39:267–75.
[32] Schroeder CM, Babcock HP, Shaqfeh ESG, Chu S. Observation of polymer conformation hysteresis in extensional flow. Science 2003;301:1515–9.
[33] Dai L, Renner CB, Doyle PS. Metastable knots in confined semiflexible chains. Macromolecules 2015;48:2812–8.
[34] Tang J, Du N, Doyle PS. Compression and self-entanglement of single DNA molecules under uniform electric field. Proc Natl Acad Sci 2011;108:16153–8 [Isotropic compression of DNA molecules was reported to generate self-entangled DNA. A comparison between unentangled and self-entangled DNA molecules undergoing re-expansion resulted in slower dynamics in the presence of topological contraints.].
[35] Renner CB, Du N, Doyle PS. Enhanced electrohydrodynamic collapse of DNA due to dilute polymers. Biomicrofluidics 2014;8:034103.
[36] Renner CB, Doyle PS. Stretching self-entangled DNA molecules in elongational fields. Soft Matter 2015;11:3105–14 [Self-entangled DNA molecules are observed to stretch in elongational fields by fundamentally different mechanisms compared to unentangled DNA. The dynamics of self-entangled DNA was also qualititatively captured using a simple, non-Brownian dumbbell model.].
[37] Renner CB, Doyle PS. Untying knotted DNA with elongational flows. ACS Macro Lett 2014;3:963–7 [Simulations of various DNA knots revealed topologically dependent transport mechanisms for knots along a polymer chain. Notably, torus knots exhibited global, sustained rotational motions, whereas non-torus knots moved primarily by self-reptation.].
[38] Yan Z-C, Costanzo S, Jeong Y, Chang T, Vlassopoulos D. Linear and nonlinear shear rheology of a marginally entangled ring polymer. Macromolecules 2016;49: 1444–53.
[39] Li Y, Hsiao K-W, Brockman CA, Yates DY, Robertson-Anderson RM, Kornfield JA, et al. When ends meet: circular DNA stretches differently in elongational flows. Macromolecules 2015;48:5997–6001 [This work focuses on the single molecule dynamics of linear and circular DNA in planar extensional flow, revealing different relaxation, steady-state extension, and transient stretching dynamics between different topologies. Ring polymers required stronger flows to stretch and exhibited less molecular individualism when compared to linear polymers.].
[40] Hsiao K-W, Schroeder CM, Sing CE. Ring polymer dynamics are governed by a coupling between architecture and hydrodynamic interactions. Macromolecules 2016;49:1961–71 [This study uses Brownian dynamics simulations to study ring polymer stretching in planar extensional flow. It was observed that stronger flows were required to stretch circular polymers, in agreement with Ref. 39. A quantitative model is derived to show that secondary hydrodynamic backflows between parallel strands of stretched rings contribute significantly to dynamics, giving rise to unexpected looped polymer conformations in the plane orthogonal to flow.].
[41] Robertson RM, Laib S, Smith DE. Diffusion of isolated DNA molecules: dependence on length and topology. Proc Natl Acad Sci 2006;103:7310–4.
[42] Serag MF, Abadi M, Habuchi S. Single-molecule diffusion and conformational dynamics by spatial integration of temporal fluctuations. Nat Commun 2014;5 [These authors report a new technique for measuring single polymer diffusion with improved accuracy and precision.].
[43] Gorczyca SM, Chapman CD, Robertson-Anderson RM. Universal scaling of crowding-induced DNA mobility is coupled with topology-dependent molecular compaction and elongation. Soft Matter 2015;11:7762–8 [The conformation and mobility of circular and linear DNA are investigated in crowded solutions mimicking intracellular environments. Although equilibrium DNA conformations are found to depend on topology, DNA mobility was independent of both length and topology above a critical degree of crowding.].
[44] Chapman CD, Gorczyca S, Robertson-Anderson RM. Crowding induces complex ergodic diffusion and dynamic elongation of large DNA molecules. Biophys J 2015; 108:1220–8.
[45] Robertson RM, Smith DE. Strong effects of molecular topology on diffusion of entangled DNA molecules. Proc Natl Acad Sci 2007;104:4824–7 [This work reports topology-dependent self-diffusion of DNA molecules, most notably revealing drastically slowed diffusion of circular polymers in an entangled linear polymer solution. These findings suggest that linear polymers thread through rings, wherein the process of releasing threaded constraints is slower than linear polymer reptation and the diffusion of pure, entangled ring polymers.].

* Of special interest.
** Of outstanding interest.

[46] Robertson RM, Smith DE. Self-diffusion of entangled linear and circular DNA molecules: dependence on length and concentration. Macromolecules 2007;40:3373–7.
[47••] Chapman CD, Shanbhag S, Smith DE, Robertson-Anderson RM. Complex effects of molecular topology on diffusion in entangled biopolymer blends. Soft Matter 2012;8:9177–82 [This work reports a systematic study of blends of entangled rings and linear polymers revealed a non-monotonic dependence of linear polymer diffusivity on blend composition. The authors propose an empirical model of variable threading between linear and circular polymers upon varying blend composition.].
[48•] Abadi M, Serag MF, Habuchi S. Single-molecule imaging reveals topology dependent mutual relaxation of polymer chains. Macromolecules 2015;48:6263–71 [This work characterizes the diffusion modes and conformational relaxation times in topologically complex entangled solutions using the methods of Ref. 42.].
[49] Laib S, Robertson RM, Smith DE. Preparation and characterization of a set of linear DNA molecules for polymer physics and rheology studies. Macromolecules 2006;39:4115–9.
[50] Robertson RM, Smith DE. Direct measurement of the confining forces imposed on a single molecule in a concentrated solution of circular polymers. Macromolecules 2007;40:8737–41.
[51] Zimmerman SB, Minton AP. Macromolecular crowding: biochemical, biophysical, and physiological consequences. Annu Rev Biophys Biomol Struct 1993;22:27–65.
[52] Tanyeri M, Schroeder CM. Manipulation and confinement of single particles using fluid flow. Nano Lett 2013;13:2357–64.
[53] Shenoy A, Rao CV, Schroeder CM. Stokes trap for multiplexed particle manipulation and assembly using fluidics. Proc Natl Acad Sci 2016.
[54] Larson RG. The structure and rheology of complex fluids. OUP USA; 1999.
[55] Subramanian G, Shanbhag S. Self-diffusion in binary blends of cyclic and linear polymers. Macromolecules 2008;41:7239–42.
[56•] Snijkers F, Pasquino R, Olmsted PD, Vlassopoulos D. Perspectives on the viscoelasticity and flow behavior of entangled linear and branched polymers. J Phys Condens Matter 2015;27:473002 [This review article critically assesses progress in all areas of the rheology of entangled branched polymers.].
[57] Seeman NC, Kallenbach NR. Design of immobile nucleic acid junctions. Biophys J 1983;44:201–9.
[58] Duckett DR, Murchie AIH, Diekmann S, von Kitzing E, Kemper B, Lilley DMJ. The structure of the Holliday junction, and its resolution. Cell 1988;55:79–89.
[59] Returning to the fold. Editorial, Nat Mater 2016;15:245.
[60••] Heuer DM, Saha S, Archer LA. Electrophoretic dynamics of large DNA stars in polymer solutions and gels. Electrophoresis 2003;24:3314–22 [Star DNA polymers are generated based on immobilized nucleic acid junctions, and electrophoresis dynamics were studied in polymer solutions and gels. Star DNA polymers are found to adopt vastly different molecular conformations in comparison to linear DNA and became trapped in gels with fixed networks.].
[61] Saha S, Heuer DM, Archer LA. Electrophoretic mobility of linear and star-branched DNA in semidilute polymer solutions. Electrophoresis 2006;27:3181–94.
[62] Saha S, Heuer DM, Archer LA. Effect of matrix chain length on the electrophoretic mobility of large linear and branched DNA in polymer solutions. Electrophoresis 2004;25:396–404.
[63•] Marciel AB, Mai DJ, Schroeder CM. Template-directed synthesis of structurally defined branched polymers. Macromolecules 2015;48:1296–303 [This work reports the graft-onto synthesis of precisely branched molecules based on DNA. This approach enables exact topological control, as well as a method for generating large branched polymers for single molecule studies.].
[64••] Mai DJ, Marciel AB, Sing CE, Schroeder CM. Topology-controlled relaxation dynamics of single branched polymers. ACS Macro Lett 2015;4:446–52 [This work provided the first single molecule studies of DNA comb polymers, focusing on conformational relaxation dynamics of branched DNA tethered to a surface. Single molecule experiments reveal a strong dependence of relaxation time on the number and position of branches along a DNA backbone.].
[65] Keshavarz M, Engelkamp H, Xu J, Braeken E, Otten MBJ, Uji-i H, et al. Nanoscale study of polymer dynamics. ACS Nano 2016;10:1434–41.